Journal of Solid State Chemistry 183 (2010) 2903–2909

Contents lists available at ScienceDirect

Journal of Solid State Chemistry

journal homepage: www.elsevier.com/locate/jssc

Exchange interaction at the interface of Fe–NiO nanocomposites

S.P. Pati, B. Bhushan, D. Das *

UGC-DAE Consortium for Scientific Research, Kolkata Centre III/LB-8, Bidhannagar, Kolkata 700 098, India

ARTICLE INFO

Article history:
Received 18 June 2010
Received in revised form
14 September 2010
Accepted 26 September 2010
Available online 1 October 2010

Keywords:
Nanocomposites
Mössbauer spectroscopy
Exchange bias
Magnetic properties

ABSTRACT

Fe–NiO nanocomposites with Fe to NiO ratio 20:80, 30:70 and 50:50 were prepared by a chemical route. X-ray diffraction and TEM measurements showed the presence of α-Fe and NiO phases in the prepared nanocomposites having an average crystallite size 17 nm. HRTEM image showed a structurally disordered phase at the Fe–NiO interface. Mössbauer spectra of the nanocomposites consist of a doublet along with a sextet corresponding to relaxed and blocked α-Fe phases, respectively. The dc magnetization measurements in field-cooled condition show a shift of hysteresis loop and an enhancement of coercive field at low temperature confirming the presence of exchange bias at Fe–NiO interfaces. The irreversibility observed in the FC and ZFC magnetization measurements also points to exchange bias effect.

1. Introduction

The study of exchange bias (EB) effect is of current interest because it plays crucial role in applications involving spin valves as well as tunnelling and storage devices [1]. It has been shown that exchange interaction at the interfaces of a composite consisting a ferromagnetic (FM) and an antiferromagnetic (AFM) component can be useful to overcome the superparamagnetic limit in FM nanoparticles [2,3]. Exchange bias effect was first observed by Meiklejohn and Bean in Co–CoO particulate system [4]. Although exchange bias effect has been widely studied in multi-layer systems [2,5,6], the polycrystalline powder systems also show considerable exchange bias effect [4,7–19]. Skumryev et al. have used the exchange bias effect to overcome the superparamagnetic limit in Co–CoO multilayer [2]. Most of the nanocomposite systems used to study the EB effect were prepared through chemical routes and are composed of a transition metal and its oxide such as Co–CoO [7,8], Ni–NiO [9,20], Mn–Mn_xO_y [10] and Fe–Fe_xO_y [11] or oxides with different oxidation states such as in CrO_2–Cr_2O_3 [12,13], Fe_3O_4–FeO [14,15] and Mn_3O_4–MnO [16]. Apart from FM–AFM interfaces, the EB effect has also been observed in samples involving a ferrimagnet (FI) and a spin glass (SG) e.g. FI–FM, FI–AFM AFM–SG, FM–SG, FI–SG, etc. [17–19]. Traditionally, nanogranular systems showing EB are obtained by subjecting FM particles to reactive treatment (partial oxidation or reduction, surface modification by chemical treatment, etc.) to obtain AFM phases. However, these methods usually give poor control of the compositional features of the final samples.

In the present paper, structural, hyperfine and magnetic properties of Fe–NiO nanocomposites prepared by a chemical route have been reported. A different approach has been adapted to get better control on the compositional features of the FM–AFM interfaces. α-Fe was chosen as the ferromagnetic phase as it is Mössbauer sensitive and has relatively small anisotropy ($K \approx 0.5 \times 10^5$ J/m^3) whereas NiO was chosen as the AFM phase because of its high Néel temperature ($T_N = 523$ K) and larger anisotropy ($K \approx 2.8 \times 10^5$ J/m^3). Due to higher anisotropy of NiO, it was expected that it could stabilize the magnetic moment of α-Fe nanoparticles over thermal fluctuation. Another advantage of choosing NiO is that since it has a high Néel temperature it may raise the blocking temperature of relaxing α-Fe nanoparticles above 300 K through the exchange bias interaction at the Fe–NiO interfaces of the nanocomposites.

2. Experimental details

The Fe–NiO nanocomposites were prepared by a two-step chemical route. In the first step, Fe and NiO nanoparticles were synthesized separately and in the second step nanocomposites were prepared by intense sonication of different weight proportions of Fe and NiO nanoparticles dispersed in propanol. For preparation of Fe nanoparticles, 5 mmol $FeCl_2 \cdot 4H_2O$ and appropriate amount of polyvinyl alcohol (PVA) was dissolved in 150 ml of Milli-Q water in a three-necked closed flask under nitrogen atmosphere. 0.5 M sodium borohydrate ($NaBH_4$) was added drop wise to the solution up to pH 9 under vigorous stirring. $NaBH_4$ was used as a reducing agent and poly vinyl alcohol (PVA) was used as a surfactant to prevent coagulation and oxidation. Precipitates so obtained were separated out, washed several

* Corresponding author. Fax: +91 33 2335 7008.
E-mail address: ddas@alpha.iuc.res.in (D. Das).

0022-4596/$ - see front matter © 2010 Elsevier Inc. All rights reserved.
doi:10.1016/j.jssc.2010.09.037

times with H_2O and propanol. Then the collected sample was dried at room temperature in vacuum and heat treated at 500 °C in a vacuum furnace for 2 h. For NiO nanoparticles, 5 mmol of $Ni(NO_3)_2 \cdot 6H_2O$ was dissolved in 150 ml of water and 0.5 M NaOH was added drop wise to the solution under vigorous stirring until pH reaches 9. The precipitate thus formed was collected, dried and heat treated at 500 °C for 2 h in open atmosphere. In the next step, total 1 g powder of Fe and NiO were dispersed in 100 ml propanol with Fe: NiO weight ratio as 50:50, 30:70 and 20:80. To break apart agglomerates of particles and to obtain a homogeneous composite, the mixture was sonicated for 1 h under nitrogen atmosphere in a sonicator operating at a frequency 33 ± 3 kHz. The particles were then filtered and dried in vacuum at room temperature. The samples were named according to iron content in them, i.e. the sample FN50 contains 50% iron.

The structural properties of the prepared nanocomposites were determined by the X-ray diffraction (XRD) technique using a Brucker D8 Advance X-ray diffractometer with a copper target ($\lambda = 0.1541838$ nm). The diffraction angles corresponding to different peaks were matched with those in standard JCPDS data files to identify the phases formed. From the broadened peaks the average crystallite sizes were determined using the Scherrer formula. A JEOL 2100 model high resolution transmission electron microscope (HRTEM) operating at 200 kV was used for imaging the nanocomposites. The room temperature Mössbauer measurements were carried out in a standard pc-based multichannel analyser with 1024 channels working in the constant acceleration mode. A 25 mCi ^{57}Co in Rh matrix was used as the radioactive source. The system was calibrated with a high purity iron foil of thickness 12 μm. The spectra thus obtained were deconvoluted using LGFIT2 programme [21]. Magnetic properties of the nanocomposites were investigated by using a vibrating sample magnetometer (VSM, Lakeshore, model 7407) and a SQUID magnetometer (Quantum Design, MPMS XL 7).

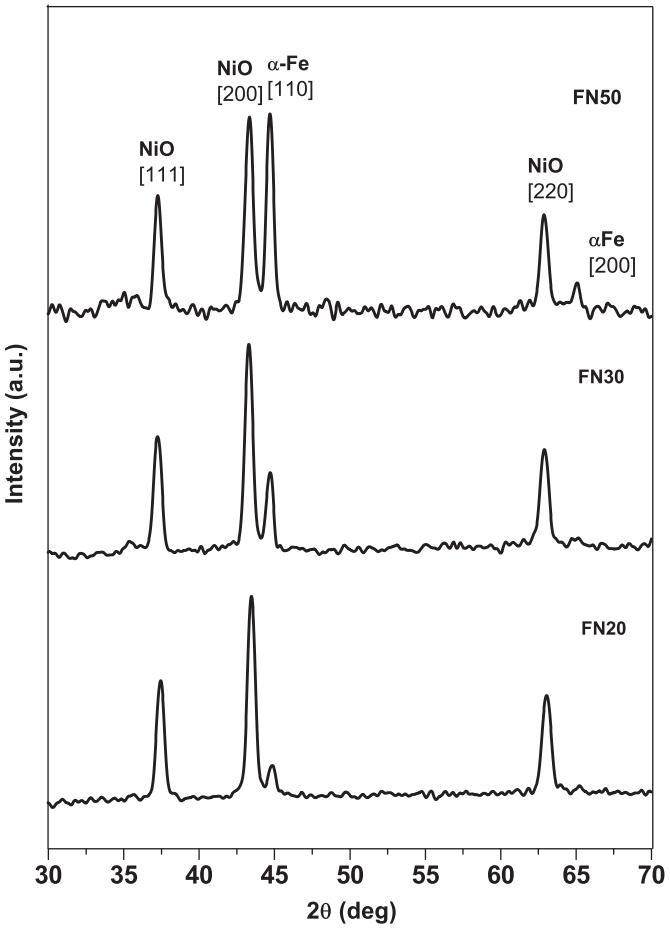

Fig. 1. X-ray diffractograms of Fe–NiO nanocomposites.

3. Results and discussions

3.1. Structural and morphological analysis

XRD patterns of all the nanocomposites are shown in Fig. 1. From the diffractograms it is clear that all the composites have both cubic α-Fe and NiO phases. The intensity of Fe [110] peak was found to decrease with decrease in iron concentration in the composites. The average crystallite size of the constituents of the nanocomposites i.e. α-Fe and NiO are calculated from the line broadening of the corresponding diffraction peaks using the Debye–Scherrer formula. The average crystallite size of α-Fe and NiO are found to 17 and 18 nm, respectively. None of the diffractograms showed the presence of α-Fe_2O_3 or any other phase of iron oxide.

In order to get more information on the material microstructures, the nanocomposites were examined by transmission electron microscopy. Fig. 2(a) shows a typical particle size distribution obtained for the sample FN20. It is evident from the figure that Fe nanoparticles (having darker contrast) are randomly distributed among the NiO nanoparticles. It is also clear from the micrograph that all the Fe and NiO nanograins form a well faceted polygonal shape, having size in the range 16–50 nm. Fig. 2(b) shows the selected area electron diffraction (SAED) pattern of the sample FN20 confirming the polycrystalline nature of the sample. The *d*-values calculated from the ring diameters confirmed the presence of both α-Fe and NiO and the corresponding crystal planes are labelled. The high resolution transmission electron micrograph (HRTEM) of the sample FN20 revealed some structurally disordered region at the Fe–NiO interface (marked by elliptic shapes in Fig. 2(c)). Such structurally disordered regions at the interface of different nanocomposite systems were also observed before [20,22]. The high velocity interparticle collision produced by ultrasonic irradiation may be a cause of this disordered interface regions [23]. In the HRTEM images long range crystalline order of NiO is not clearly visible while that of Fe is clearly observed. Fig. 2(d) shows a typical high resolution image of a section of Fe–NiO nanocomposite where inter planer spacing of Fe is clearly visible corresponding to [110] plane.

3.2. Hyperfine analysis

The magnetic anisotropy energy of a particle is responsible for holding the magnetic moment along a certain direction. In the case of nanoparticles, the magnetic anisotropy energy decreases with decreasing particle size and below a critical size becomes comparable with the thermal energy. At this stage the anisotropy energy is insufficient to hold the magnetic moment along a certain direction, thus the magnetic moment flips randomly due to thermal energy. Therefore, a nanoparticle loses its stable magnetic order and becomes superparamagnetic. To stabilize the magnetic order of a relaxing ferromagnet, it should be exchange coupled with an antiferromagnet having higher anisotropy energy. Such exchange-coupled system can be useful to overcome the superparamagnetic limit of ferromagnetic nanoparticles [2,3]. In order to study the effect of exchange bias on superparamagnetic nanoparticles, Mössbauer study at room temperature was carried out on the nanocomposites.

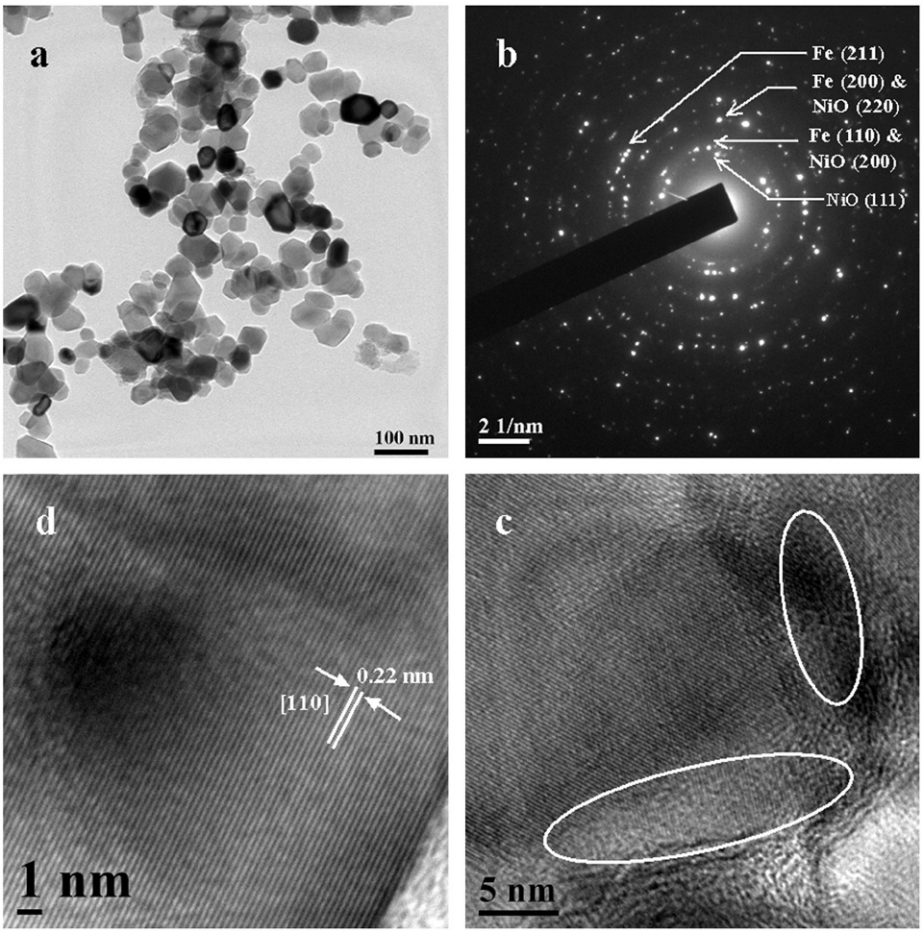

Fig. 2. (a) TEM image showing the particle distribution of FN20. (b) SAED pattern of FN20. (c) The HRTEM image showing the disordered regions (marked in elliptic shape). (d) The HRTEM image showing Fe [110] planes.

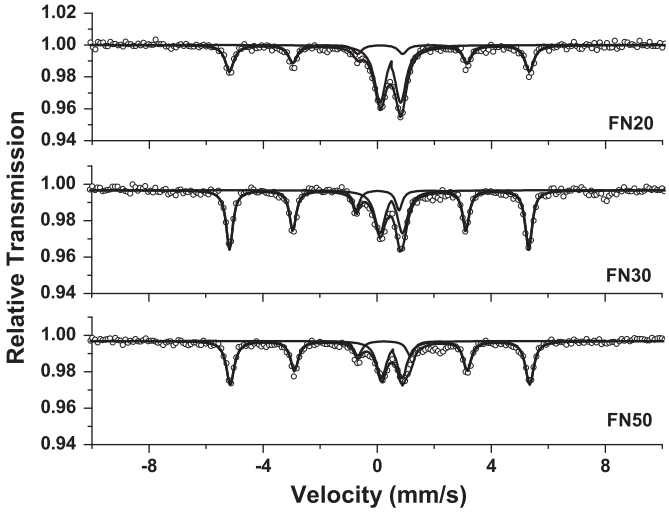

Fig. 3. Mössbauer spectra of Fe–NiO nanocomposites.

Fig. 3 shows room temperature Mössbauer spectra of all the Fe–NiO nanocomposites. All the spectra consist of a sextet and a doublet. The hyperfine parameters obtained after fitting the spectra are tabulated in Table 1. The sextets having very low isomer shifts and quadrupole splittings with internal magnetic field ~33 T are assigned to α-Fe nanoparticles in the blocked state [24]. The sextet may have resulted due to two reasons.

Table 1
Mössbauer parameters of all Fe–NiO nanocomposites.

Sample ID		I.S[a] (mm/s) (±0.01 mm/s)	QS[b] (mm/s) (±0.01 mm/s)	H_{int}[c] (T) (±0.3 T)	Area (%)
FN20	S[d]	0.09	0.02	32.7	41
	D[e]	0.46	0.71	–	59
FN30	S	0.06	0.01	32.6	63
	D	0.50	0.79	–	37
FN50	S	0.10	0.03	32.6	65
	D	0.52	0.72	–	35

[a] IS: isomer shift.
[b] QS: quadrupole splitting.
[c] H_{int}: internal magnetic field.
[d] S: sextet.
[e] D: doublet.

The Fe nanoparticles, which are located at the Fe–NiO interfaces, experience strong exchange coupling with the ordered magnetic moment of NiO nanoparticles. As NiO have comparatively large magnetic anisotropy, it can hold the magnetic moment of Fe nanoparticles in a specific direction. So these particles can overcome the thermal fluctuation and become magnetically stable. Secondly, the fraction of Fe nanoparticles having size greater than the critical size (~25 nm) of becoming super-paramagnetic at room temperature can also give a sextet pattern. The central doublets appeared in the spectra are assigned to Fe

nanoparticles undergoing superparamagnetic relaxation. The Fe nanoparticles that are away from the Fe–NiO interfaces experience very weak exchange force thus become unstable and undergo spontaneous relaxation. The Fe nanoparticles that are in contact with the disordered NiO interfaces (as seen in HRTEM micrograph) also experience very little exchange force and thus remain superparamagnetic giving a doublet Mössbauer pattern. Finer Fe particles having size less than 25 nm will undergo spontaneous relaxation and give a doublet pattern. A close inspection of the spectra reveals that the intensity of the doublet increases as the amount of Fe in the composites decreases. Since all the composites are having similar particle size distribution one can not explain this observation by assuming higher fraction of smaller particles in the composite with lower concentration of Fe. As the concentration of Fe in the composite decreases, the strength of dipolar interaction among them should also decrease and the doublet intensity is expected to increase. Thus weak dipolar interaction among ferromagnetic α-Fe nanoparticles may be another cause of the observed doubles at room temperature.

3.3. Magnetization analysis

DC magnetization measurements were performed on all Fe–NiO nanocomposites to investigate their magnetic properties. In order to observe exchange bias (EB), the system needs to be cooled below Néel temperature (T_N) of the AFM component in the presence of a magnetic field and the Curie temperature of the FM component should be higher than T_N. As a result, the AFM anisotropy exerts a microscopic torque on FM spins located near the AFM–FM interface. Thus the field needed to reverse completely a FM layer magnetization will be larger if it is in contact with an AFM material, because an extra field is needed to overcome the microscopic torque on FM spins. The material behaves as if there is an extra internal biasing field that manifests in a shift in the ferromagnetic hysteresis loop in the field axis.

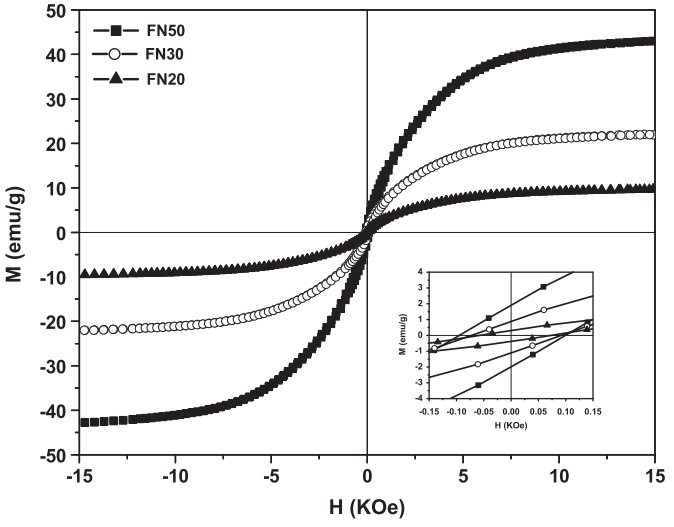

Fig. 4. Room temperature *M–H* curves of all Fe–NiO nanocomposites; the inset shows enlarged central portions.

The *M–H* loops at room temperature of all the samples are shown in Fig. 4 and the inset shows magnified view of the central portion of the loops. It is clear from the nature of the loops that the nanocomposites are magnetically soft. Calculated saturation magnetization, M_S (at 15 kOe), remanent magnetization, M_R (positive value at $H=0$) and coercive field, H_C (average of $+H_C$ and $-H_C$) are shown in Table 2. M_S, M_R and H_C were found to decrease with decrease in Fe concentration in the samples. This can be explained by considering the fact that strength of dipolar interaction among α-Fe nanoparticles reduces as concentration of Fe decreases in the nanocomposites. Mössbauer results as discussed in the previous section also support this fact as the relative area of the doublet increases with decrease in Fe concentration. The central part of the magnetic hysteresis loops for all samples measured at 80 K for ZFC and FC conditions in a 14 kOe applied field, cooled from 300 K, are shown in Fig. 5(a)–(c). It is evident that FC hysteresis loops do not keep good central symmetry. The shift in the hysteresis loop may be quantified through the exchange field parameter $H_E=-(H_{right}+H_{left})/2$, whereas the coercive field is defined as $H_C=(H_{right}-H_{left})/2$, H_{right} and H_{left} being the points where the loop intersects the field axis. The values of H_C, M_S, M_R and H_E obtained from the $M-H$ loops are given in Table 2. The observed value of exchange bias field for all samples is low. This could be due to the reason that the magnetic anisotropy of NiO is not large enough to prevent the magnetic moment reversal of α-Fe nanoparticles on application of a magnetic field in reverse direction. The enhancement of coercivity as seen in all nanocomposites in field cooling condition is also an evidence of the presence of exchange bias in the system [25]. It is to be noted that highest exchange bias field has been observed in the sample FN30 (20 ± 3 Oe) which has 30% Fe concentration in contrast to 20% and 50% in the samples FN20 and FN50, respectively. This indicates that the magnitude of EB field does not depend on Fe concentration in the nanocomposites, rather it depends on the Fe–NiO interface area which is more in case of FN30 due to random distribution Fe and NiO particles in the nanocomposites.

The temperature dependent magnetization curves of the sample FN50 in zero field cooled (ZFC) and field cooled (FC) conditions with an applied field 100 Oe are shown in Fig. 6. It can be seen that the ZFC and FC magnetization curves show a distinct irreversible behaviour, and this irreversibility persists beyond 300 K. The observed irreversibility in the ZFC and FC curves strongly points to the presence of a relaxed magnetic phase in the sample. The structurally disordered regions at the interfaces as confirmed by HRTEM studies may be the reason for such irreversible magnetic behaviour [20,22]. At room temperature, the local anisotropy of disordered NiO component is small but it increases as the temperature is lowered. This results in freezing of AFM spins in the anisotropy direction. As a result of exchange bias the FM spins at the interface also gradually go to a blocked state. Thus, the irreversibility as observed in the present case

Table 2
Magnetization data of all samples taken at room temperature and at 80 K in FC condition.

Sample ID	At room temperature			Field cooled to 80 K at 14 kOe field			
	H_c (Oe)	M_s (emu/g)	M_r (emu/g)	H_c (Oe)	M_s (emu/g)	M_r (emu/g)	H_E (Oe)
FN20	65 ± 5	9.8	0.3	99 ± 5	10.1	0.6	15 ± 3
FN30	83 ± 5	22.2	0.9	144 ± 5	23.1	1.8	20 ± 3
FN50	97 ± 5	43.2	1.9	150 ± 5	40.5	2.7	12 ± 3

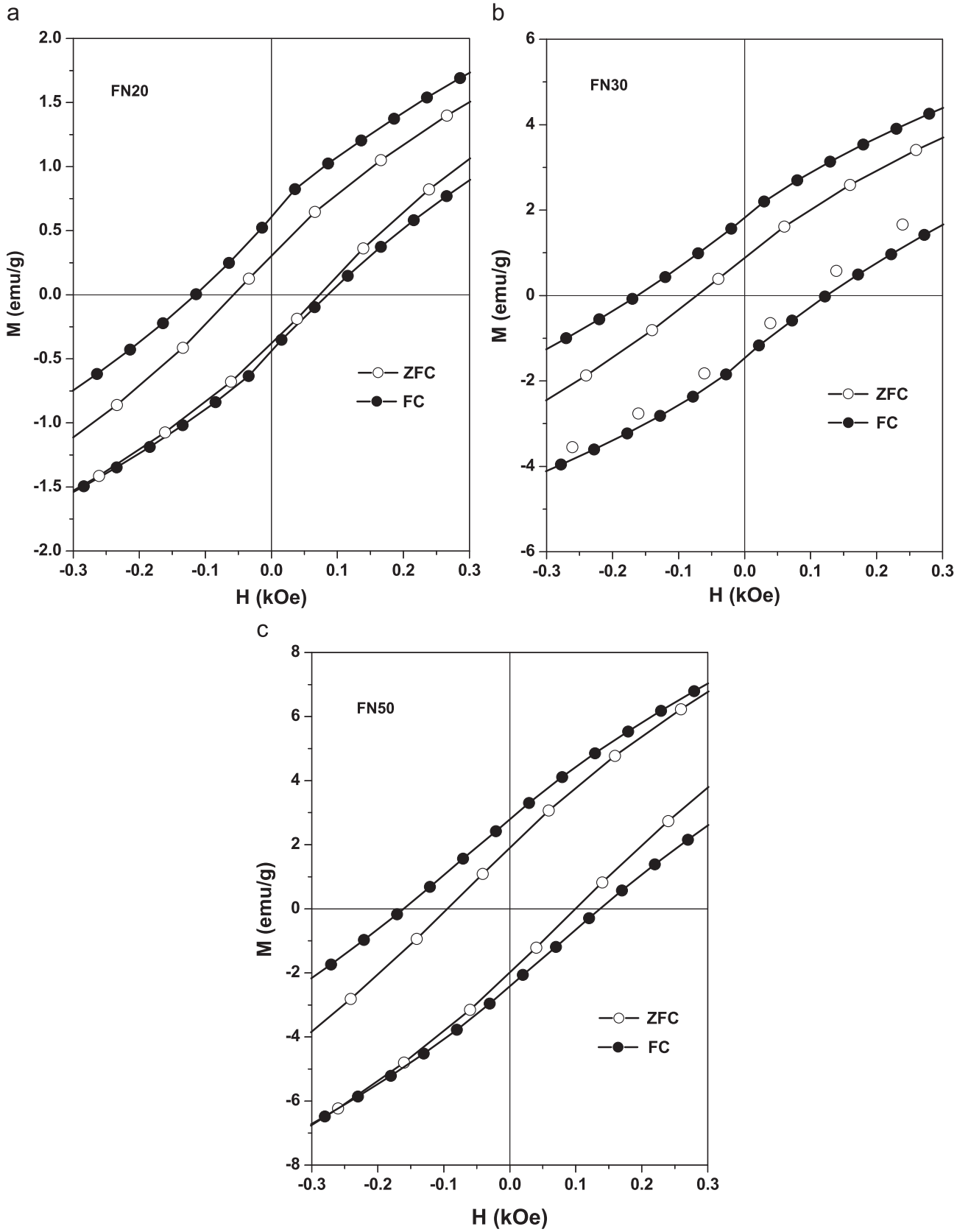

Fig. 5. Magnified central portion of *M–H* loops under FC (applied cooling field of 14 kOe) and ZFC conditions of (a) FN20, (b) FN30 and (c) FN50 nanocomposite recorded at 80 K.

is a consequence of strong exchange coupling across the interface boundaries of the FM and AFM components in the nanocomposites. A close inspection of the ZFC curve reveals that there is a change of slope in the temperature range 70–130 K. This can be due to transition of the disordered Fe spins at the interfaces to a spin glass (SG) like frozen state as the temperature

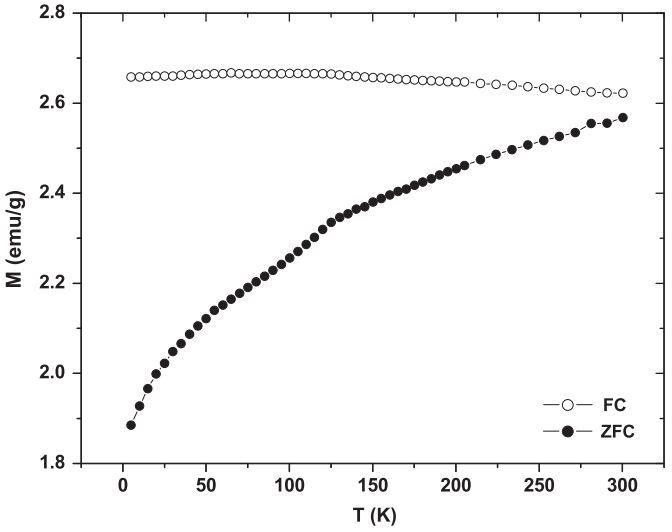

Fig. 6. $M-T$ curves of FN50 nanocomposite at an applied field of 100 Oe.

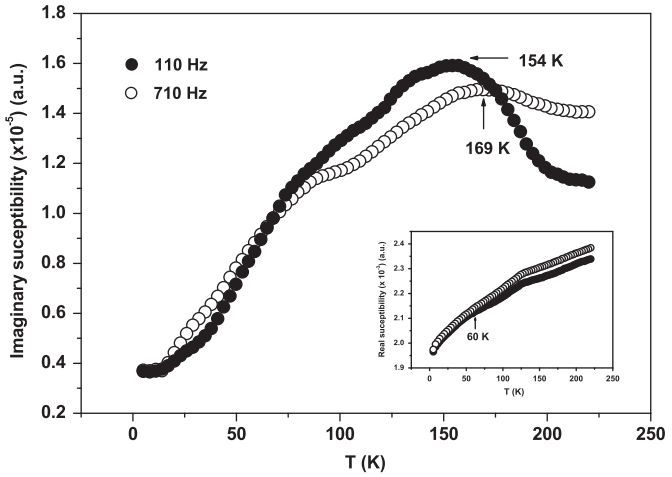

Fig. 7. Temperature dependent out of phase component of ac susceptibility of FN50. The inset shows the variation of the in-phase component with temperature.

of the nanocomposite is reduced. The spins of the disordered NiO component freeze along the random anisotropy direction at low temperature and consequently the exchange coupled Fe spins freeze, giving rise to the observed SG behaviour. Another point to be noted is that the ZFC and FC curves tend to merge at a temperature beyond 300 K. Apparently the system has a blocking temperature (T_B) above the room temperature. This can be attributed to high ($\sim$523 K) Néel temperature of NiO that has effectively raised the superparamagnetic blocking temperature of the nanocomposites above room temperature.

To get more information on the magnetic properties of the nanocomposites, the real (in-phase) and imaginary (out-of-phase) components of the ac magnetic susceptibility were measured as a function of temperature at different frequencies. Data were collected while cooling the samples from 220 down to 5 K. Fig. 7 shows the results obtained with a driving field of amplitude $H_0=3.5$ Oe, oscillating at frequencies 110 and 710 Hz. The in-phase susceptibility component, χ' (see inset of Fig. 7) is seen to increase continuously with increase in temperature. As temperature is increased above 60 K, the in-phase susceptibility component is seen to depend strongly on frequency, which is reflected in the marked diverging behaviour. The out of phase component, χ'', exhibits a pronounced peak at around 154 K for 110 Hz, below which it falls rapidly. With increase of frequency to 710 Hz, this peak shifts towards higher temperature region i.e. to 169 K. This behaviour is attributed to the spin glass like phase, formed at the AFM–FM interface [26]. This fact is also supported by temperature dependent dc magnetization measurement that shows a change of slope around 130 K (Fig. 6).

4. Conclusion

To conclude, Fe–NiO nanocomposites with Fe concentration varying from 20 to 50 wt% were prepared successfully by a soft chemical route. XRD and SAED results confirmed the formation of pure phase nanocomposites. The HRTEM image confirmed the presence of structurally disordered regions in the FM–AFM interfaces. Mössbauer spectroscopy confirmed the presence of α-Fe nanoparticles in a blocked state giving typical sextet pattern. Weak dipolar interaction among Fe nanoparticles, Fe nanoparticles at the disordered NiO interfaces and Fe nanoparticles away from the ordered NiO interface were argued to be possible causes of appearance of doublets in the Mössbauer spectra. The observed hysteresis loop shift along the field axis and enhancement in coercivity in field-cooled condition confirmed the presence of exchange bias in the nanocomposites. Irreversibility in the FC and ZFC curves confirmed strong FM–AFM exchange coupling in the Fe–NiO nanocomposite system. A change of slope in the ZFC curve around 130 K has been assigned to transition to a spin glass like state which is confirmed by ac susceptibility measurements.

Acknowledgments

The authors are grateful to Dr. S. Das, Jadavpur University, Kolkata for XRD measurements. Thanks are also due to Dr. K. Mondal, S N Bose National Centre for Basis Sciences, Kolkata for VSM measurements. One of the authors (B. Bhushan) thanks CSIR, Govt. of India for the award of senior research fellowship.

References

[1] G.A. Printz, Science 282 (1998) 1660.
[2] V. Skumryev, S. Stoyanov, Y. Zhang, G. Hadjipanayis, D. Givord, J. Nogues, Nature 423 (2003) 850.
[3] J. Eisenmenger, I.K. Schuller, Nat. Mater. 2 (2003) 437.
[4] W.P. Meiklejohn, C.P. Bean, Phys. Rev. 102 (1956) 1413.
[5] J. Nogues, I.K. Schuller, J. Magn. Magn. Mater. 192 (1999) 203.
[6] A.E. Berkowitz, K. Takano, J. Magn. Magn. Mater. 200 (1999) 552.
[7] S. Gangopadhyay, G.C. Hadjipanayis, C.M. Sorensen, K.J. Klabunde, J. Appl. Phys. 73 (1993) 6964.
[8] J.B. Tracy, D.N. Weiss, D.P. Dinega, M.G. Bawendi, Phys. Rev. B 72 (2005) 064404.
[9] I.S. Lee, N. Lee, J. Park, B.H. Kim, Y.W. Yi, T. Kim, T.K. Kim, I.H. Lee, S.R. Paik, T. Hyeon, J. Am. Chem. Soc. 128 (2006) 10658.
[10] P.Z. Si, D. Li, J.W. Lee, C.J. Choi, Z.D. Zhang, D.Y. Geng, E. Bruck, Appl. Phys. Lett. 87 (2005) 133122.
[11] R.K. Zheng, G.H. Wen, X.X. Zhang, Phys. Rev. B 69 (2004) 214431.
[12] M.H. Yu, P.S. Devi, L.H. Lewis, P. Oouma, J.B. Parise, R.J. Gambino, Mater. Sci. Eng. B 103 (2003) 262.
[13] R.K. Zheng, H. Liu, X.X. Wang, Appl. Phys. Lett. 84 (2004) 702.
[14] F.X. Redl, C.T. Black, G.C. Papaefthymiou, R.L. Sandstrom, M. Yin, H. Zheng, C.B. Murria, S.P. O'Brien, J. Am. Chem. Soc. 126 (2004) 14583.
[15] C.J. Bae, Y. Hwang, J. Park, K. An, Y. Lee, J. Lee, T. Hyeon, J.G. Park, J. Magn. Magn. Mater. 310 (2007) E806.
[16] G. Salazar-Alvarez, J. Sort, S. Surinach, M.D. Baro, J. Nogues, J. Am. Chem. Soc. 129 (2007) 9102.
[17] P.J. Vander Zaag, R.M. Wolf, A.R. Ball, C. Bordel, L.F. Feiner, R. Jungblut, J. Magn. Magn. Mater. 148 (1995) 346.
[18] R.K. Zheng, G.H. Wen, K.K. Fung, X.X. Zhang, J. Appl. Phys. 95 (2004) 5244.

[19] L.D. Bianco, D. Fiorani, A.M. Testa, E. Bonetti, L. Signorini, Phys. Rev. B 70 (2004) 052401.
[20] L.D. Bianco, F. Boscherini, M. Tamisari, F. Spizzo, M.V. Antisari, E. Piscopiello, J. Phys. D: Appl. Phys. 41 (2008) 134008.
[21] E.V. Meerwall, Comput. Phys. Commun. 9 (1975) 117.
[22] Z.M. Tian, S.L. Yuan, S.Y. Yin, L. Liu, J.H. He, H.N. Duan, P. Li, C.H. Wang, Appl. Phys. Lett. 93 (2008) 222505.
[23] K.S. Suslick, Science 247 (1990) 1439.
[24] R.S. Preston, S.S. Hanna, J. Heberle, Phys. Rev. 128 (1962) 2207.
[25] J. Nogues, J. Sort, V. Langlais, V. Skumryev, S. Surinach, J.S. Munoz, M.D. Baro, Phys. Rep. 422 (2005) 65.
[26] E. Bonetti, L.D. Bianco, D. Fiorani, D. Rinaldi, R. Caciuffo, A. Hernando, Phys. Rev. Lett. 83 (1999) 14.